

Cite this: *RSC Adv.*, 2018, 8, 10437

Cipadessains A–K, eleven limonoids from the fruits of *Cipadessa cinerascens*†

Dong-Mei Sun, Fa-Liang An, Shan-Shan Wei, Yan-Qiu Zhang, Xiao-Bing Wang, Jun Luo* and Ling-Yi Kong*

Received 24th January 2018
Accepted 26th February 2018

DOI: 10.1039/c8ra00728d

rsc.li/rsc-advances

Eleven new mexicanolide-type limonoids, cipadessains A–K (1–11), were isolated from the fruits of *Cipadessa cinerascens* (Pellegr.) Hand.-Mazz. Their planar structures were determined based on IR, UV, 1D and 2D NMR spectra and HRESIMS data. The absolute configuration of **1** was elucidated by single-crystal X-ray diffraction using mirror Cu K α radiation, and that of compounds **2**–**8** were determined by ECD analysis. Two mexicanolides bearing methoxybutenolide moiety originated from the furan ring **3** and **6**, showed significant cytotoxicity against HepG2 cell line with IC₅₀ values of 5.23 \pm 0.12, 8.67 \pm 1.02 μ M, respectively; and NO inhibitory activities in LPS-activated RAW 264.7 macrophages at nontoxic concentration (IC₅₀ 5.79 \pm 0.18, 6.93 \pm 0.89 μ M, respectively).

Introduction

Cipadessa cinerascens (Pellegr.) Hand.-Mazz is a species of *Cipadessa* genus and known as ‘Ya Luo Qing’ or ‘Lao Ya Fan’ by the Dai.¹ Its roots and leaves have been used in Chinese folk medicine for the treatment of rheumatism, stomachache, dysentery, malaria, scald, and skin itch.^{1–3} Previous reports demonstrated that terpenoids, flavonoids, steroids, and limonoids are the main bioactive constituents of *Cipadessa* genus.^{2,3} Among those compounds, limonoids have become a point of interest in the field of natural products, because of its diverse skeletons (mexicanolides, methyl angolensates, trijugins, and cipadesins) and various biological effects such as cytotoxic, insecticidal, antioxidant, and trypanocidal activities.^{2–6} Previous studies on *Cipadessa* genus focused on their leaves, roots, barks and stems.^{4–15} To our knowledge, there have been few phytochemical investigations on the fruits of *Cipadessa* species. In continuing search for new bioactive limonoids, 11 new mexicanolide limonoids with various modified furan rings, cipadessains A–K (1–11), were isolated from the fruits of *C. cinerascens*. All the isolates were evaluated for NO inhibitory activities in LPS activated RAW 264.7 macrophages and cytotoxicity against HepG2 cell line. In this paper, we describe the isolation, identification of 1–11, as well as their bioactivity screening.

Results and discussion

Cipadessain A (**1**), was isolated as white powder, and assigned to a molecular formula of C₃₂H₄₀O₉ on the basis of HRESIMS at *m/z* 591.2560 [M + Na]⁺ (calcd C₃₂H₄₀O₉Na, 591.2565), corresponding with 13 degrees of unsaturation. Its IR absorption bands at 3460 and 1728 cm^{−1} showed the presence of hydroxyl and carbonyl functionalities. The NMR data (Table 1) revealed the characteristic resonances for β -substituted furan ring [δ_{H} 7.93 (H-21), 7.45 (H-23), and 6.50 (H-22), δ_{C} 143.4 (C-23), 142.4 (C-21), 120.5 (C-20), 109.7 (C-22)], four tertiary methyls (δ_{H} 1.42, 1.11, 0.85, 0.83); a characteristic downfield H-17 signal (δ_{H} 5.43); a ketone carbonyl (δ_{C} 217.3), three ester carbonyls (δ_{C} 175.1, 168.6, 167.2) and two unsaturated bonds (δ_{H} 6.90, 5.39; δ_{C} 139.6, 137.5, 127.6, 125.6). In the HMBC spectrum (Fig. 2), both angular methyls (C-28, C-29) were attached to C-4 (δ_{C} 38.7), were elucidated by the cross peaks from H₃-28 (δ_{H} 0.83) to C-29 (δ_{C} 20.3), C-5 (δ_{C} 41.8) and C-3 (δ_{C} 77.6), and from H₃-29 (δ_{H} 0.85) to C-28 (δ_{C} 22.9), C-5 (δ_{C} 41.8) and C-3 (δ_{C} 77.6); a C-6/7 esterified appendage (δ_{H} 3.74; δ_{C} 52.3, 175.1) was easily verified by the HMBC cross peaks from H₂-6 (δ_{H} 2.98, 2.40) to C-5 (δ_{C} 41.8), C-7 (δ_{C} 175.1) and from OCH₃ (δ_{H} 3.74) to C-7 (δ_{C} 175.1). From cross peaks of H-3 (δ_{H} 4.83) to C-5 (δ_{C} 41.8), C-30 (δ_{C} 125.6), of H-30 (δ_{H} 5.39) to C-9 (δ_{C} 63.9), C-1 (δ_{C} 217.3), and of H₃-19 (δ_{H} 1.42) to C-1 (δ_{C} 217.3), C-5 (δ_{C} 41.8), and C-9 (δ_{C} 63.9), the characteristic [3, 3, 1] A/B ring system could be elucidated.¹⁶ Furthermore, the HMBC correlations from H-17 (δ_{H} 5.43) to C-12 (δ_{C} 45.4), C-18 (δ_{C} 21.4), C-14 (δ_{C} 45.4), from H-15b (δ_{H} 2.73) to C-13 (δ_{C} 37.4), C-16 (δ_{C} 168.6), from H-15a (δ_{H} 2.85) to C-8 (δ_{C} 137.5), from H₃-18 (δ_{H} 1.11) to C-17 (δ_{C} 76.7), C-14 (δ_{C} 45.4) indicated the ring C/D in **1**.^{14,16} These aforementioned data strongly suggested **1** was a B,D-*seco* mexicanolide-type limonoid,^{7,19} typical constituent of *Cipadessa* genus.

State Key Laboratory of Natural Medicines, Department of Natural Medicinal Chemistry, China Pharmaceutical University, 24 Tong Jia Xiang, Nanjing 210009, People's Republic of China. E-mail: luojun1981ly@163.com; cpu_lykong@126.com; Fax: +86-25-8327-1405; Tel: +86-25-8327-1405

† Electronic supplementary information (ESI) available: HRESIMS, 1D and 2D NMR spectra of compounds 1–11 and ECD spectrum of 1–8 are available as supporting information. CCDC 1815118. For ESI and crystallographic data in CIF or other electronic format see DOI: 10.1039/c8ra00728d

Table 1 ^1H NMR and ^{13}C NMR spectral data of compounds 1–4 in CDCl_3 (δ in ppm, J in Hz)

Position	1^a		2^a		3^a		4^a	
	δ_{H}	δ_{C}	δ_{H}	δ_{C}	δ_{H}	δ_{C}	δ_{H}	δ_{C}
1		217.3		216.9		217.2		216.6
2	3.56, dd (8.8, 7.7)	48.9	3.50, t (9.7)	48.9	3.50 ^b	49.2	3.56, t (10.0)	48.8
3	4.83, d (9.4)	77.6	4.81, d (9.5)	77.2	4.83, d (9.2)	77.3	4.83, d (9.3)	77.3
4		38.7		38.7		38.9		38.7
5	3.49, d (10.4)	41.8	3.39, dd (7.9, 3.8)	41.4	3.51 ^b	40.4	3.37, d (9.5)	41.7
6	2.40, dd (16.8, 10.8)	32.2	2.38, m	33.0	2.36, dd (17.3, 10.4)	33.1	2.39, dd (17.0, 9.5)	32.8
	2.98, d (16.8)		2.38, m		2.48, d (17.3)		2.23, d (17.0)	
7		175.1		174.1		173.3		174.5
8		137.5		141.2		138.0		137.5
9	2.19, d (9.8)	63.9	2.72, dd (12.2, 5.5)	53.0	2.20 ^b	56.5	2.25 ^b	56.4
10		49.7		50.1		50.6		50.0
11	4.60, td (10.4, 4.6)	65.8	1.64 ^b	20.2	1.73 ^b	21.1	1.76, m	20.5
			2.07, dd (13.0, 4.1)		2.29, td (13.2, 3.5)		2.07, m	
12	1.39, d (11.8)	45.4	1.33, d (13.5)	28.6	1.43, td (14.0, 3.5)	34.8	1.59, m	34.2
	1.82, d (11.8)		1.98, dd (13.5, 4.1)		1.91, d (14.0)		1.83, m	
13		37.4		41.3		36.8		37.3
14	2.24, d (5.8)	45.4		73.4	2.22 ^b	45.4	2.24 ^b	45.4
15	2.85, dd (18.8, 5.8)	30.0	2.99, d (18.0)	39.2	2.79, m	29.2	2.80, m	29.5
	2.73, d (18.8)		2.92, d (18.0)		2.78, m		2.79, m	
16		168.6		168.6		167.8		167.0
17	5.43, s	76.7	5.66, s	77.4	5.54, s	76.6	5.73, s	78.1
18	1.11, 3H, s	21.4	1.08, 3H, s	15.9	1.00, 3H, s	22.8	1.07, 3H, s	21.9
19	1.42, 3H, s	18.7	1.16, 3H, s	15.9	1.16, 3H, s	15.7	1.16, 3H, s	15.8
20		120.5		120.1		136.1		164.1
21	7.93, s	142.4	7.84, s	142.4		168.2	4.98, dd (18.0, 2.8)	72.3
22	6.50, s	109.7	6.49, s	110.0	7.23, s	147.8	6.21, d (1.08)	118.7
23	7.45, s	143.4	7.42, s	143.0	5.80, s	102.4		172.9
28	0.83, 3H, s	22.9	0.78, 3H, s	22.5	0.79, 3H, s	22.6	0.78, 3H, s	22.5
29	0.85, 3H, s	20.3	0.82, 3H, s	20.6	0.81, 3H, s	20.9	0.82, 3H, s	20.4
30	5.39, td (7.5, 11.7)	125.6	5.63, d (6.8)	124.5	5.34, d (6.6)	123.4	5.35, d (6.9)	124.3
7-OCH ₃	3.74, 3H, s	52.3	3.71, 3H, s	52.3	3.64, 3H, s	52.1	3.69, 3H, s	52.5
23-OCH ₃					3.58, 3H, br s	57.6		
1'		167.2		176.7		167.3		167.1
2'		127.6	2.62, m	33.9		127.8		127.7
3'	6.90, m	139.6	1.15, 3H ^b	19.2	6.91, m	139.3	6.88, m	139.4
4'	1.80, 3H, s	11.9	1.17, 3H ^b	18.6	1.84, 3H, s	12.0	1.82, 3H, m ^b	12.0
5'	1.68, 3H, d (7.1)	14.7			1.82, 3H, d (7.3)	14.8	1.82, 3H, m ^b	14.9

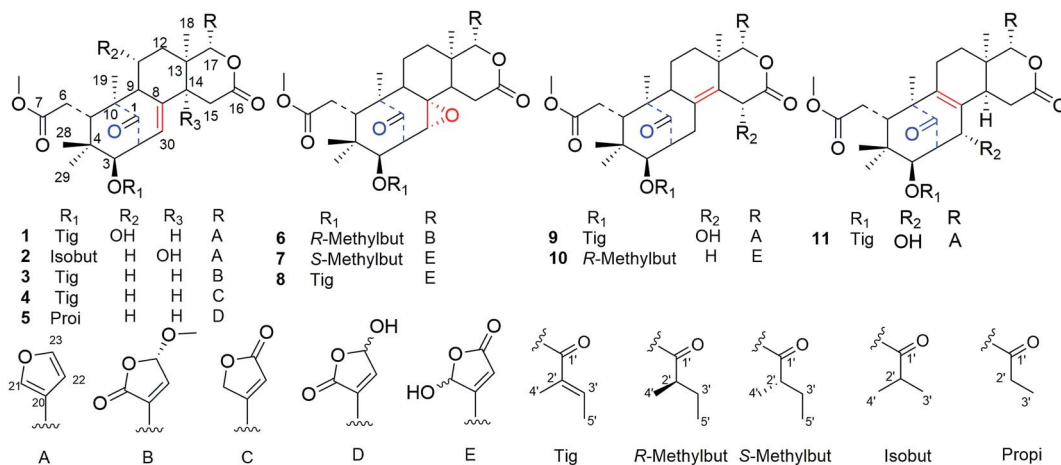
^a ^1H (500 MHz) NMR data of compounds. ^b Signals were overlapped.

Fig. 1 Chemical structures of cipadessains A–K (1–11).



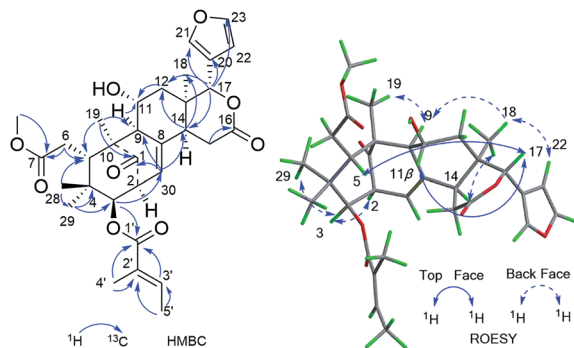


Fig. 2 Key HMBC and ROESY correlations of compound 1.

Furthermore, the existence of $\Delta^{8,30}$ double bond was determined by the HMBC correlations from H-30 (δ_{H} 5.39) to C-9 (δ_{C} 63.9) and C-14 (δ_{C} 45.4), and from H-2 (δ_{H} 3.56) to C-1 (δ_{C} 217.3), C-30 (δ_{C} 125.6). The correlation from H-3 (δ_{H} 4.83) to C-1' (δ_{C} 167.2) of the tigloyl moiety [δ_{H} 6.90 (H-3'), 1.80 (H-4'), 1.68 (H-5'); δ_{C} 167.2 (C-1'), 139.6 (C-3'), 127.6 (C-2'), 14.7 (C-5'), 11.9 (C-4')] showed the presence of a tigloyl group at C-3. The NMR data of **1** were similar to those of 6-desoxyiswietenine,¹⁷ except for the additional of a hydroxyl group at C-11 in **1**. This inference was verified by the HSQC correlation of H-11 (δ_{H} 4.60) with C-11 (δ_{C} 65.8) and HMBC correlations from H-9 (δ_{H} 2.19) and H-12 (δ_{H} 1.82, 1.39) to C-11 (δ_{C} 65.8). Thus, the planar structure of **1** was determined as shown in Fig. 1.

The ROESY correlations between H-17 (δ_{H} 5.43)/H-11 (δ_{H} 4.60), H-5 (δ_{H} 3.49)/H-28 (δ_{H} 0.83) suggested these protons were the same configuration (Fig. 2). In turn, the ROESY correlations between H-2 (δ_{H} 3.56)/H-3 (δ_{H} 4.83), H-3 (δ_{H} 4.83)/H-29 (δ_{H} 0.85), H-14 (δ_{H} 2.24)/H-19 (δ_{H} 1.42) and H-9 (δ_{H} 2.19)/H-19 (δ_{H} 1.42) revealed that they were co-facially oriented. Accordingly, the structure of **1** was proposed as shown. Fortunately,

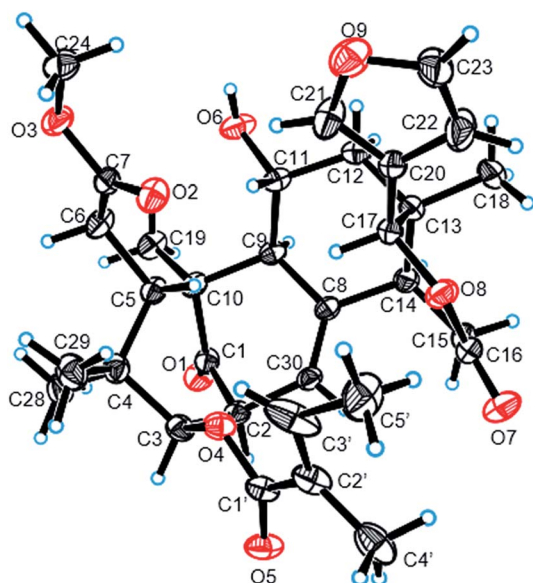


Fig. 3 Single-crystal X-ray diffraction (Cu K α radiation) of compound 1.

compound **1** was recrystallized in the $\text{CH}_2\text{Cl}_2/\text{MeOH}$ (1 : 1) mixture to yield prisms. On the basis of single-crystal X-ray diffraction data (CCDC 1815118), the absolute stereochemistry of **1** was elucidated to be 2*S*, 3*R*, 5*S*, 9*S*, 10*S*, 11*R*, 13*S*, 14*R*, 17*S* (Fig. 3). Finally, the structure of **1**, with a $\Delta^{8,30}$ double bond and a 11-hydroxyl group, was established as depicted in Fig. 1.

Compound **2**, was obtained as a colorless needles, which had a sodium adduct ion peak at m/z 579.2568 $[\text{M} + \text{Na}]^+$ in the HRESIMS spectrum corresponding to a molecular formula of $\text{C}_{31}\text{H}_{40}\text{O}_9$. The NMR spectroscopic data of **2** (Table 1) exhibited closed similarity to those of **1**. In comparison to **1**, the correlations from H-3-3' (H-3-4') to C-1' (δ_{C} 176.7) and from C-2' (δ_{C} 33.9), H-3 (δ_{H} 4.81) to C-1' (δ_{C} 176.7) in the HMBC spectrum indicated the presence of an isobutyryloxy group at C-3 in **2** instead of a tigloyl group in **1**. An upfield shift at δ_{C} 20.2 (Δ - 45.6 ppm) of C-11 and a downfield shift at δ_{C} 73.4 (Δ + 28.0 ppm) of C-14 in the ^{13}C NMR spectrum of **2** as compared with the corresponding signals of **1** implied that the hydroxyl group was located at C-14. The deduction was supported by the HMBC correlations of C-14 (δ_{C} 73.4) and H-15 (δ_{H} 2.99, 2.92), H-17 (δ_{H} 5.66), H-30 (δ_{H} 5.63). The α -oriented of OH-14 was determined by comparison of NMR data of **2** with those of two known compounds Khasenegasin D and Khasenegasin E.¹⁴ Therefore, the structure of **2** was established as shown (Fig. 1).

Compound **3** was isolated as a white amorphous powder and showed the HRESIMS ion peak at m/z 621.2669 $[\text{M} + \text{Na}]^+$ (calcd for $\text{C}_{33}\text{H}_{42}\text{O}_{10}\text{Na}$, 621.2670). The spectroscopic data of **3** were similar to those of 6-desoxyiswietenine,¹⁷ except for the presence of 23-methoxybutenolide ring moiety in **3** instead of the β -substituted furan moiety as found in 6-desoxyiswietenine. This was confirmed by the HMBC correlations of OCH_3 -23 (δ_{H} 3.58)/C-23 (δ_{C} 102.4); of H-23 (δ_{H} 5.80)/C-21 (δ_{C} 168.2), C-20 (δ_{C} 136.1); of H-22 (δ_{H} 7.23)/C-23 (δ_{C} 102.4), C-20 (δ_{C} 136.1), C-21 (δ_{C} 168.2); of H-17 (δ_{H} 5.54)/C-21 (δ_{C} 168.2), C-20 (δ_{C} 136.1). Thus, the planar structure of **3** was identified as shown. The relative configuration of **3** was mainly elucidated by its ROESY data and comparison of its NMR spectroscopic data with those of similar reported compounds.¹⁷ The correlations between H-17/H-11b (δ_{H} 2.29), H-17/H-15b (δ_{H} 2.78), H-17/H-5 (δ_{H} 3.51), indicated these groups were on the same side of the structure, and they were assigned as β -configuration. Correlations of H-3-19 (δ_{H} 1.16)/H-9 (δ_{H} 2.20)/H-2 (δ_{H} 3.50), H-9/H-3 (δ_{H} 4.83)/H-29 (δ_{H} 0.81), H-3/H-14 (δ_{H} 2.22) and cross peaks of OCH_3 -23/ CH_3 -18 revealed that these protons were α -oriented. Hence, the structure of **3** was elucidated as shown in Fig. 4 and named cipadessain C.

Compound **4**, a white, amorphous powder, displayed a molecular formula $\text{C}_{32}\text{H}_{40}\text{O}_9$, on the basis of its HRESIMS ion at m/z 591.2568 $[\text{M} + \text{Na}]^+$, $\text{C}_{32}\text{H}_{40}\text{O}_9\text{Na}$, calcd 591.2565). The ^1H and ^{13}C NMR data (Table 1) of **3** and **4** were almost the same except for signals of the E ring. The appearance of α,β -unsaturated- γ -lactone ring portion linked to C-17 in **4** was determined by the HMBC correlations between H-17 (δ_{H} 5.73)/C-20 (δ_{C} 164.1), C-21 (δ_{C} 72.2), C-22 (δ_{C} 118.7) and H-2-21 (δ_{H} 4.98)/C-20 (δ_{C} 164.1), C-22 (δ_{C} 118.7), C-23 (δ_{C} 172.9). The ROESY correlations were observed between H-17 (δ_{H} 5.73)/H-5 (δ_{H} 3.37), H-5/H-11b (δ_{H} 2.07), H-5/H-28 (δ_{H} 0.78), H-3-29 (δ_{H} 0.82)/H-3 (δ_{H} 4.83), H-3/H-2 (δ_{H} 3.56) suggesting the relative configuration of



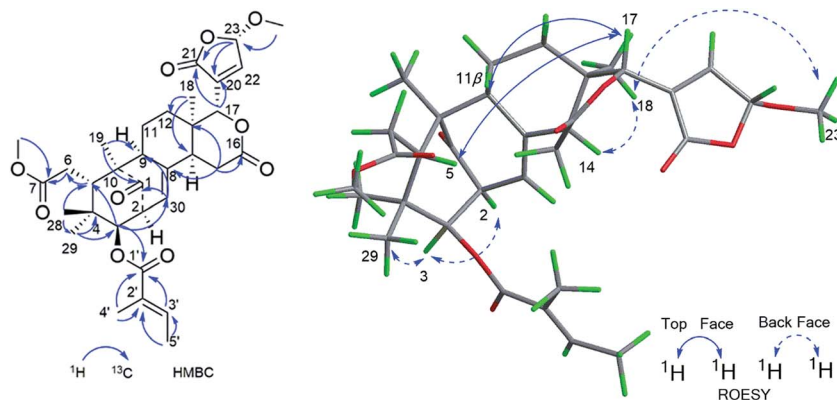


Fig. 4 Key HMBC and ROESY correlations of compound 3.

4 was similar to that of **3**. Thus, the structure of **4** was finally determined and represented in Fig. 1.

Compound **5**, a white amorphous powder, afforded a molecular formula of $C_{30}H_{38}O_{10}$ as assigned by the (+)-HRESIMS ion peak at m/z 581.2353 $[M + Na]^+$ (calcd 581.2357) and the ^{13}C -NMR data. The NMR data (Table 2) of **5** resembled those of 3-de(2-methylbutanoyl)-3-propanoylcipadesin¹⁸ except for the additional presence of 21-hydroxybutenolide unit attached to C-17 in **5**. This was confirmed by the cross peaks from H-17 (δ_H 5.60) to C-20 (δ_C 135.1/135.0), C-22 (δ_C 149.8/149.6) in the HMBC spectrum. The appearance of pairs of proton and carbon resonances in the NMR spectra of **5** indicated the presence of epimers at C-21.¹⁹ Thus, based on these data, the planar structure of **5** was established.

Compound **6** gave a molecular formula of $C_{33}H_{44}O_{11}$ from the positive ion peak at m/z 639.2771 $[M + Na]^+$ (calcd for $C_{33}H_{44}O_{11}Na$, 639.2776). The 1D and 2D NMR data (Table 2) of **6** were similar to those of 2'*R*-cipadesin A,⁷ a mexicanolide-type limonoid with a $\Delta^{8,30}$ epoxide ring from *Cipadessa fruticosa*. The structures **6**, featuring 23-methoxybutenolide ring in the C-17 side-chain, was verified by the key HMBC cross peaks of OCH_3 -23 (δ_H 3.62/3.56)/C-23 (δ_C 103.1); H-23 (δ_H 5.82/5.78)/C-21 (δ_C 169.8), C-20 (δ_C 133.7); H-22 (δ_H 7.28)/C-17 (δ_C 76.5). In the ROESY spectrum, the cross peak of H-23 (δ_H 5.82) to H-17 (δ_H 5.10) confirmed the β -configuration of H-23 in **6**. The detailed analysis of the ROESY correlations based on the general rule,⁷ in which the cross peaks of H₃-4' (δ_H 1.25) to H-15b (δ_H 2.85) and H-30 (δ_H 3.31), of H-2' (δ_H 2.56) to H-30 (δ_H 3.31), of H₃-5' (δ_H 0.97) and H₃-29 (δ_H 0.79), revealed the remaining relative configurations of **6** (Fig. 5) were identical to those of 2'*R*-cipadesin A.

Compound **7**, a white amorphous powder, exhibited the molecular formula of $C_{32}H_{42}O_{11}$ based on the pseudo-molecular ion peak at m/z 625.2620 $[M + Na]^+$ (calcd for $C_{32}H_{42}O_{11}Na$, 625.2619). The 1H and ^{13}C -NMR data of **7** were closely comparable to those of **6** for rings A–D (Table 2), while the 23-methoxybutenolide group was absent, and concomitantly a γ -hydroxybutenolide group. This difference was supposed by the broad singlet signals of H-21 at δ_H 6.32/6.14 and H-22 at δ_H 6.34/6.22 and by carbon signals at δ_C 162.7/160.4 (C-20), 98.7/97.7 (C-21), 122.5/121.8 (C-22), 169.4/169.0 (C-23). The α -configuration of epoxide ring at C-8/C-30 was supposed from the coupling

constant value of H-30 ($J = 2.5$ Hz).²⁰ The appearance of pairs of most proton and carbon resonances in the NMR spectra (Table 2) of **7** identified the presence of C-21 epimers. Thus, compound **7** was elucidated as a mexicanolide-type limonoid bearing γ -hydroxybutenolide group. According to the general ruler,⁷ the ROESY correlations between H₃-5' (δ_H 0.97) and H-30 (δ_H 3.30), between H-2' (δ_H 2.55) and H-15 α (δ_H 3.50), between H₃-4' (δ_H 1.24) and H₃-29 (δ_H 0.78) confirmed its relative configurations were as the same as that of cipadesin A.

The molecular formula of **8** was determined to be $C_{32}H_{40}O_{11}$ from the HRESIMS peak at m/z 623.2464 (calcd for $C_{32}H_{40}O_{11}Na$, 623.2463), 2 mass units less than **7**. The NMR data of **8** (Table 2) exhibited overall similarity to those of **7**, but revealed the presence of a tigloxyl moiety instead of a 2-methylbutyryl moiety attached to C-3, this was proved by the HMBC correlations of H₃-4' (δ_H 1.91) to C-1' (δ_C 167.0), C-3' (δ_C 140.6/140.2), of H₃-5' (δ_H 1.90) to C-2' (δ_C 127.6/127.2), of H-3 (δ_H 5.03) to C-1' (δ_C 167.0). Therefore, the planar structure of **8** was assigned as shown. The α -configuration of epoxide ring at C8/30 was determined by the coupling constant value of H-30 ($J = 2.3$ Hz).²⁰ The relative configuration of the tigloxyl moiety at C-3 was β -oriented according to the observed ROESY correlations between H-3 and H-2, and the coupling constant value of H-3 ($J = 9.4$ Hz).²¹ The appearance of pairs of most proton and carbon resonances in the NMR spectra (Table 2) of **8** suggested the presence of C-21 epimers. Its relative configurations were as the same as that of **7** by ROESY experiment. Therefore, the structure of **8** was elucidated as shown in Fig. 1.

The similar electronic circular dichroism spectra of **1**–**8** (see S1 in ESI†) indicated that the basic skeletons of these compounds possessed absolute configurations as Fig. 1.

Compound **9** was isolated as a white powder. Its molecular formula, $C_{32}H_{40}O_9$ was deduced from the HRESIMS data (m/z 567.2597 $[M - H]^-$, calcd for $C_{32}H_{39}O_9$, 567.2600). Analysis of its NMR spectra indicated that **9** was an analogue of proceranolide.²² A proton signal at δ_H 4.97 was correlated with a carbon signal at δ_C 65.4 in HSQC spectrum and the HMBC correlation from the hydroxyl group (δ_H 3.18 br s) to C-15 (δ_C 65.4) indicated that the hydroxyl group was located at C-15. Furthermore, a tigloxyl moiety was located at C-3', which was confirmed by the HMBC correlation from H-3 (δ_H 4.89) to C-



Table 2 ^1H NMR and ^{13}C NMR spectral data of compounds 5–8 in CDCl_3 (δ in ppm, J in Hz)

Position	5 ^a		6 ^a		7 ^a		8 ^a	
	δ_{H}	δ_{C}	δ_{H}	δ_{C}	δ_{H}	δ_{C}	δ_{H}	δ_{C}
1		217.3/217.2		214.3		213.9		214.2
2	3.49, m	48.8	3.57 ^b	48.9	3.58, dd (9.5, 3.2)	48.9	3.66, d (9.3, 2.4)	49.3/49.1
3	4.75, d (9.2)	77.4 ^b	5.09, d (9.2)	77.1	5.09, dd (9.5, 2.4)	77.1	5.03, d (9.3)	78.1/77.5
4		38.6		39.5		39.5/39.3		39.4/39.2
5	3.39, d (10.0)	40.7/40.7	3.21, t (5.0)	42.6	3.20, d (9.3)	42.9/42.6	3.27, d (9.4)	43.0/42.6
6	2.43, dd (17.1, 5.8)	33.1/33.0	2.35, d (5.0)	33.1	2.36	33.3	2.40, d (16.6)	33.2
	2.37 ^b		2.35, d (5.0)		2.33		2.39, dd (16.6, 9.7)	
7		173.9/173.6		174.3		174.8		174.9
8		137.9/137.8		60.6		60.1		60.1
9	2.23 ^b	56.3/56.2	1.90 ^b	56.1	1.94 ^b	54.9/54.6	1.94, m	54.8/54.4
10		50.5/50.2		48.4		48.3/48.2		48.3/48.2
11	1.73, br s	20.9	1.76, m	19.5	1.78, m	19.5	1.85, m	19.8/19.6
	2.23 ^b		1.88, m		1.93 ^b		2.01, m	
12	1.92, d (14.0)	34.5	1.13 ^b	32.8	2.13, d (13.9)	33.1	2.10, m	33.3
	1.44, m		2.25, d (16.3)		1.39, m		1.41, m	
13		36.8/36.7		36.8		36.5/36.4		36.3/26.2
14	2.24 ^b	45.5	1.49 ^b	46.4	1.56, m	46.6/46.5	1.56, dd (12.7, 4.0)	46.5/46.1
15	2.84, m	29.6	3.76, m	34.7	3.50, dd (16.4, 13.7)	33.6/33.5	3.40, dd (16.1, 13.6)	33.1
	2.84, m		2.85, dd (15.5, 3.7)		2.84, dd (16.4, 4.3)		2.77, dd (16.5, 4.0)	
16		169.0/169.0		171.3		170.7		170.4
17	5.60, s	77.2	5.10, s	76.5	5.30, br s/5.15, br s	79.2/78.4	5.30, br s/5.12, br s	78.8
18	1.06/1.04, 3H, s	23.0	1.04, 3H, s	26.5	1.23/1.22, 3H, br s	16.3/16.2	1.20/1.07, 3H, br s	26.2/24.5
19	1.14, 3H, s	15.7/15.7	1.06, 3H, s	15.8	1.08/1.06, 3H, br s	26.7/26.2	1.08, 3H, br s	16.4
20		135.1/135.0		133.7		162.7		162.7/160.2
21		168.6		169.8	6.32, br s/6.14, br s	98.7/97.7	6.22, br s/6.12, br s	98.8/97.7
22	7.35/7.34, br s	149.8/149.6	7.28, s	148.8	6.33, br s/6.22, br s	122.5/121.8	6.30, br s	122.4/121.3
23	6.18/6.17, br s	97.1/96.7	5.82, br s/5.78, br s	103.1		169.4/169.0		169.1
28	0.76, 3H, s	22.5	0.81, 3H, s	21.2	0.81, 3H, s	20.9/20.9	0.83, 3H, s	23.1/23.0
29	0.79, 3H, s	21.0/20.9	0.79, 3H, s	22.5	0.78, 3H, s	22.7	0.82, 3H, s	21.0
30	5.33, d (6.5)	123.3/123.3	3.31, br s	63.7	3.30, d (2.5)	63.6/63.5	3.20, d (2.2)	63.7/63.4
7-OCH ₃	3.66/3.64, 3H, br s	52.4/52.3	3.72, 3H, s	52.5				
23-OCH ₃			3.62, br s/3.56, br s	57.8	3.72, 3H, s	52.8/52.6	3.74, 3H, s	52.8/52.7
1'		174.3/174.2		175.8		176.1/175.9		167.0
2'	2.39 ^b	27.2/27.2	2.56, m	41.7	2.55, m	41.5/41.3		127.6/127.2
3'	1.12, d (7.5)	9.0	1.77, m	26.8	1.74, m	26.5	7.03, m	140.6/140.3
			1.54, m		1.52, m			
4'			1.25, 3H, d (7.0)	17.5	1.24, 3H, d (7.0)	17.3/17.3	1.91, 3H, m ^b	12.5
5'			0.97, 3H, t (7.4)	12.0	0.97, 3H, t (7.4)	11.9/11.8	1.90, 3H, m ^b	14.9

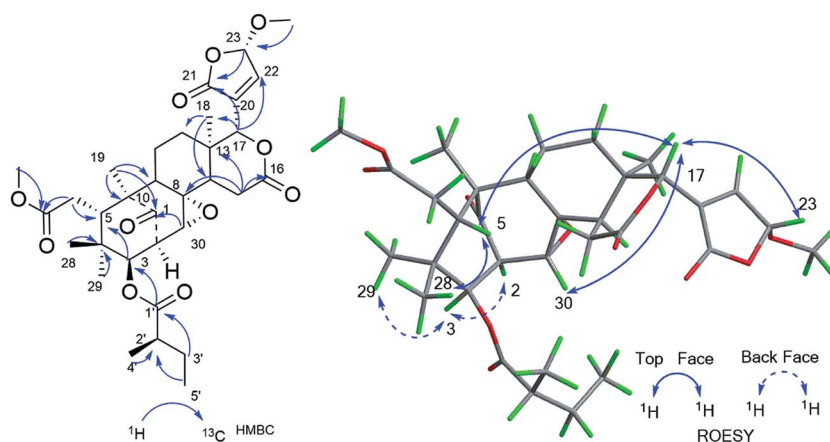
^a ^1H (500 MHz) NMR data of compounds. ^b Signals were overlapped.

Fig. 5 Key HMBC and ROESY correlations of compound 6.



1' (δ_{C} 167.2). In the ROESY spectrum, the H-15 (δ_{H} 4.97) was correlated with H-17 (δ_{H} 5.54), which suggested the H-15 was β -oriented. The other configurations of **9** were similar to that of proceranolide by ROESY spectroscopic analysis.

Compound **10**, was isolated as a white powder and its molecular formula $\text{C}_{32}\text{H}_{42}\text{O}_{10}$ was determined by the molecular ion peak at m/z 609.2675 (calcd for $\text{C}_{32}\text{H}_{42}\text{O}_{10}\text{Na}$, 609.2670) in the HRESIMS. The 1D and 2D NMR data indicated that **10** was also a mexicanolide-type limonoid bearing a γ -hydroxylbutenolide unit as **8**. A comparison of their NMR data (Table 3) revealed the main differences being the presence of the $\Delta^{8,14}$ double bond and the absence of the $\Delta^{8,30}$ epoxide ring. The conclusion was confirmed from the HMBC correlations of H-15b (δ_{H} 3.46) to C-8 (δ_{C} 129.2/128.9), of H-30b (δ_{H} 2.12) to C-14 (δ_{C} 130.8/130.5), of H-2 (δ_{H} 3.19) to C-8 (δ_{C} 129.2/128.9). Moreover, the tigolyl group was replaced by the *R*-methylbutyryl at C-3 in **10**, which can be proved

from the H-3 (δ_{H} 4.97) to C-1' (δ_{C} 176.3). The appearance of pairs of proton and carbon resonances in the NMR spectra of **10** indicated that the presence of epimers at C-21. Therefore, the structure of **10** was shown in Fig. 1. The relative structure of **10** was displayed by the ROESY experiment and general ruler.⁷

Compound **11**, was isolated as white and amorphous powder, shown as a positive HRESIMS ion peak at m/z 591.2562 ($[\text{M} + \text{Na}]^+$, calcd for $\text{C}_{32}\text{H}_{40}\text{O}_9\text{Na}$ 591.2565). The ^1H and ^{13}C -NMR data of **11** (Table 3) suggested that its structure was closely related to that of khasengasin N with $\Delta^{8,9}$ double bond.¹⁴ The only difference between **11** and khasengasin N was that a hydroxyl group linked to C-3 as found in khasengasin N was replaced by a tigloxyl group [δ_{H} 1.89 (s), δ_{H} 1.86 (d, $J = 7.1$ Hz) and 6.92 (m)] in **11**. Further, it was evidenced by HMBC correlation of H-3 (δ_{H} 5.17) to C-1' (δ_{C} 167.0) of the tigloxyl group. The relative configuration of **11** was assigned by the ROESY

Table 3 ^1H NMR and ^{13}C NMR spectral data of compounds **9–11** in CDCl_3 (δ in ppm, J in Hz)

Position	9^a		10^b		11^a	
	δ_{H}	δ_{C}	δ_{H}	δ_{C}	δ_{H}	δ_{C}
1		217.7		217.5/217.3		213.4
2	3.26, m	48.4	3.19, m	48.1	3.19, dd (7.9, 1.9)	57.0
3	4.89, m	79.3	4.97, d (9.8)	78.0/77.9	5.17, d (7.9)	77.1
4		38.8		38.4/38.2		38.4
5	3.37, dd (11.0, 1.5)	40.7	3.11, d (10.7)	41.4/41.2	2.83, t (6.0)	48.4
6	2.42, d (16.5, 11.0) 2.37, d (16.5)	33.4	2.45, m 2.36, m	33.9	2.29, d (6.0)	32.4
7		174.7		176.3/175.7		174.1
8		135.7		129.2/128.9		130.7
9	2.11, d (6.6)	51.9	2.05 ^c	51.3		142.1
10		53.6		53.1/52.8		50.9
11	1.75, m 1.89, m	18.7	1.79, m 1.94, m	18.7/18.6	2.03, m 2.38, m	21.6
12	1.00 1.78, m	28.6	1.99, m 1.27, m	28.6	1.58 ^c 1.51 ^c	29.1
13	1.02, m	38.8		39.1		35.8
14		135.0		130.8/130.5	2.45 ^c	38.2
15	4.97, s	65.4	3.77, m 3.46, d (21.0)	32.9	2.80, dd (14.0, 3.0) 2.41, d (14.0)	31.4
16		174.5		168.7/168.1		172.7
17	5.54, s	81.9	5.62, br s/5.35, br s	79.7	4.91, s	81.3
18	1.02, 3H, s	16.9	1.08, 3H, s	17.4	0.74, 3H, s	20.4
19	1.18, 3H, s	16.7	1.17, 3H, s	16.9	1.08, 3H, s	17.2
20		120.6		162.8		120.8
21	7.62, s	142.0	6.10, s	98.9/98.0	7.43, s	140.5
22	6.51, s	110.0	6.30, s	122.8/122.1	6.40, s	109.8
23	7.42, s	143.0		169.6/159.4	7.43, s	143.4
28	0.76, 3H, s	20.4	0.68, 3H, s	23.5	1.14, 3H, s	26.5
29	0.83, 3H, s	23.9	0.81, 3H, s	20.6	0.89, 3H, s	25.9 ^c
30	2.99, dd, (15.9, 1.9) 2.30, dd, (15.9, 6.6)	34.6	2.72, d (15.0) 2.12, d (6.0)	33.1	4.54, br s	71.4
7-OCH ₃	3.73, 3H, s	52.6	3.71, 3H, s	52.8/52.2	3.69, 3H, s	52.2
15-OH	3.18, br s					
1'		167.2		176.3		167.0
2'		129.4	2.40, m	41.3		128.5
3'	6.90, m	138.6	1.73, dt (20.0, 7.0) 1.51, dt (14.0, 7.0)	27.3	6.92, m	139.1
4'	1.87, 3H, m	12.5	1.21, 3H, m	16.2	1.89, 3H, s	12.5
5'	1.79, 3H, d (7.0)	14.6	0.91, 3H, dd (7.1, 5.5)	11.3	1.86, 3H, d (7.1)	14.9

^a ^1H (500 MHz) NMR data of compounds. ^b ^1H (600 MHz) NMR data of compound. ^c Signals were overlapped.



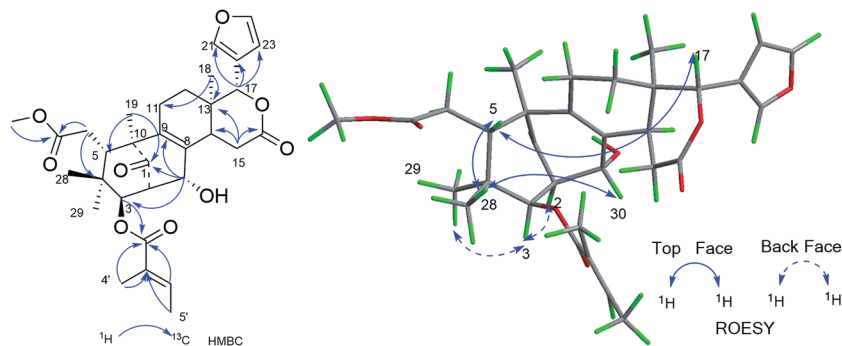


Fig. 6 Key HMBC and ROESY correlations of compound 11.

Table 4 Cytotoxicity and NO inhibition activities of compounds 1–11^{a,b}

Compounds	NO inhibition RAW 264.7 macrophages	Cytotoxicity (HepG2)
3	5.79 ± 0.18	5.23 ± 0.12
4	23.90 ± 2.1	>50
6	6.93 ± 0.89	8.67 ± 1.02
7	20.54 ± 0.63	>50
L-NMMA ^c	41.88 ± 0.91	—
Doxorubicin ^c	—	1.04 ± 0.37

^a Values were expressed as the means ± SD based on three independent experiments. ^b Compounds 1,2,5,8–11 were inactive. ^c Positive controls.

experiment, in which key cross-peaks between H-17/H-5, H-5/H-30 indicated H-30 to be β -oriented (Fig. 6). Therefore, the structure of 11 was demonstrated as shown in Fig. 1.

All the isolates were evaluated for their cytotoxicity against HepG2 cancer cell line with doxorubicin as the positive control. As shown in Table 4, compounds 3 and 6 showed significant cytotoxic activities. These isolates were further tested for their inhibitory effects on NO production of LPS-activated RAW 264.7 macrophages with *N*-monomethyl-L-arginine as the positive control (IC₅₀ 41.88 ± 0.91 μ M). The results showed that compounds 3 and 6 exhibited significant NO inhibitory activities with IC₅₀ values of 5.79 ± 0.18 μ M, 6.93 ± 0.89 μ M, respectively. On the contrary, those mexicanolides bearing complete furan moiety or hydroxybutenolide furan moiety were inactive (1, 2, 5, 8–11). According to the continuing study,^{14–16} the modified furan moiety may play important role on the bioactivity of these limonoids.

Conclusions

In summary, eleven new mexicanolide-type limonoids, cipadessains A–K (1–11) were isolated from the fruits of *Cipadessa cinerascens*. Their structures were elucidated on the NMR data and HRESIMS. The absolute configuration of 1 was determined by X-ray diffraction. In bioactivity screening, two mexicanolides (3 and 6) bearing methoxybutenolide moiety originated from the furan ring showed significant cytotoxicity activities against HepG2 cell line and NO inhibitory activities in LPS-activated RAW 264.7 macrophages, which were more excellent than

those limonoids with complete furan moiety or hydroxybutenolide furan moiety. This finding adds the complexity and diversity of mexicanolide-type limonoids in *Cipadessa cinerascens*. It's worthy of paying more attention to the cytotoxicity activities against HepG2 cell line of the limonoids with modified furan rings from the *Cipadessa* genus.

Experimental

General experimental procedures

UV and IR were recorded on a Shimadzu UV-2450 spectrophotometer (Shimadzu, Tokyo, Japan) and Bruker Tensor 27 spectrometer (Bruker, Karlsruhe, Germany), optical rotations were measured on a JASCO P-1020 polarimeter (Jasco, Tokyo, Japan). ECD spectra were obtained on a JASCO J-810 spectropolarimeter (Jasco, Tokyo, Japan) respectively. 1D and 2D NMR spectra were measured by a Bruker AVIII-600 and AVIII-500 NMR instrument at 600 and 500 MHz (¹H), 150 MHz (¹³C) and 125 MHz (¹³C) in CDCl₃. HRESI mass spectra were conducted on an Agilent 6520B UPLC-Q-TOF mass spectrometer (Agilent Technologies, Santa Clara, CA, USA). MCI gel (Mitsubishi Chemical Corp., Tokyo, Japan), MPLC (Beijing H&E Co., Ltd., Beijing, China), and RP-C₁₈ (40–63 μ m, Fuji), silica gel (Qingdao Haiyang Chemical Co., Ltd.) were used as column chromatography. Preparative HPLC was performed on a Shimadzu LC-6AD instrument with a SPD-10A detector using a shim-pack reversed-phase C₁₈ column (20 × 200 mm, 10 μ m). Analytical HPLC was carried out on an Agilent 1260 Series instrument with a DAD detector using a shim-pack VP-ODS column (250 × 4.6 mm, 5 μ m). All solvents used were analytical grade (Jiangsu Hanbon Science and Technology Co., Ltd.). The mouse macrophage cell line RAW264.7 and human hepatocellular carcinoma (HepG2) cell were obtained from the Cell Bank of the Shanghai Institute of Cell Biology and Biochemistry, Chinese Academy of Sciences (Shanghai, China). All cells were cultured in Dulbecco's modified Eagle medium (DMEM, GIBCO Invitrogen Corp., Carlsbad, CA, USA) with 10% FBS, penicillin (100 U ml^{−1}), and streptomycin (100 μ g ml^{−1}) in a humidified atmosphere with 5% CO₂ at 37 °C.

Plant material

The air-dried fruits of *Cipadessa cinerascens* (Pellegr) Hand.-Mazz (Meliaceae) were collected from Xishuangbanna,



Yunnan province, People's Republic of China, in July 2013, and authenticated by Professor Mian Zhang, Research Department of Pharmacognosy, China Pharmaceutical University. A voucher specimen (no. 2015-CCHM) has been deposited in the Department of Natural Medicinal Chemistry, China Pharmaceutical University.

Extraction and isolation

The dried and powdered fruits of *Cipadessa cinerascens* (5.0 kg) were extracted by refluxing with 95% ethanol (25 L \times 4), for 4 h, 4 h, 4 h, 3 h. The ethanol extract was concentrated under reduced pressure to afford the crude extract (637 g), it was suspended in H₂O (1.5 L) and partitioned sequentially with petroleum ether (PE), CH₂Cl₂, EtOAc. The oily PE and CH₂Cl₂ part were subjected to a silica gel column gradient eluted with CH₂Cl₂/MeOH (150 : 1 to 0 : 100) to afford collect six fractions A–F by TLC analysis. Fraction C (120 g) was run on a D101-macroporous absorption resin, eluted with EtOH/H₂O (30%, 50%, 70%, and 90%, v/v) to give six sub-fractions (C₁–C₆) monitored by HPLC. Fr. C₃ (12.8 g) was chromatographed on an ODS-C₁₈ column eluted with MeOH/H₂O (30 : 70 to 100 : 0) to obtain fourteen sub-fractions (C₃A–C₃N). Fraction C₃A was subjected to an ODS-C₁₈ column eluted with MeOH/H₂O (40 : 60, v/v) to obtain ten sub-fractions (C₃A₁–C₃A₁₀). C₃A₅ was purified by semi-preparative HPLC yielding **5** (2.2 mg). Fraction C₃F was applied to a silica gel column (CH₂Cl₂/MeOH; 100 : 1 to 0 : 100) to give five sub-fractions (C₃F₁–C₃F₅). Fraction C₃F₂ (102 mg) was separated by the semi-preparative HPLC (MeOH/H₂O; 65 : 35, v/v, 10 mL min^{−1}) to yield **3** (5.2 mg). Using the same purification procedures, fraction C₃E yielded **4** (2.3 mg), **7** (2.1 mg) and **10** (8.6 mg). Fraction C₃I was subjected to a Sephadex LH-20 gel, using CH₂Cl₂/MeOH (1 : 1) as the eluent, to obtain three sub-fractions, C₃I₁–C₃I₃. C₃I₂ was separated by the semi-preparative HPLC (MeOH/H₂O; 65 : 35, v/v, 10 mL min^{−1}) to obtain **8** (1.8 mg). Fraction C₃K (2.01 g) was subjected to MPLC to give six sub-fractions (C₃K₁–C₃K₆). Fraction C₃K₁ was repeatedly chromatographed over semi-preparative HPLC (MeCN/H₂O; 50 : 50, v/v, 10 mL min^{−1}) to afford **1** (2.2 mg), **2** (2.0 mg), **9** (4.5 mg), **11** (4.3 mg) in turn. Fraction C₃K₃ (350 mg) was subjected to silica gel column (CH₂Cl₂/MeOH; 100 : 1 to 0 : 100), further purified by the semi-preparative HPLC (MeCN/H₂O; 55 : 45) to obtain **6** (1.8 mg).

Cipadessain A (1). Colorless crystals (MeOH : CH₂Cl₂ = 1 : 1); $[\alpha]_D^{25}$ −47.6 (c 0.10, MeOH); UV (MeOH) λ_{\max} (log ϵ) 229 (3.58) nm; ECD (MeOH, $\Delta\epsilon$) 200 (−14.074), 239 (+1.894), 294 (−4.559) nm; IR (KBr) ν_{\max} 3451, 2922, 1640, 1384 cm^{−1}; ¹H and ¹³C NMR data, see Table 1; HRESIMS m/z 591.2560 [M + Na]⁺ (calcd for C₃₂H₄₀O₉Na, 579.2565).

Cipadessain B (2). Colorless crystals (MeOH : CH₂Cl₂ = 1 : 1); $[\alpha]_D^{25}$ −119.3 (c 0.13, MeOH); UV (MeOH) λ_{\max} (log ϵ) 227 (3.58) nm; ECD (MeOH, $\Delta\epsilon$) 200 (−11.079), 212 (+4.854), 293 (−2.852) nm; IR (KBr) ν_{\max} 3452, 1730, 1640, 1384 cm^{−1}; ¹H and ¹³C NMR data, see Table 1; HRESIMS m/z 579.2568 [M + Na]⁺ (calcd for C₃₁H₄₀O₉Na, 579.2565).

Cipadessain C (3). White powder; $[\alpha]_D^{25}$ −44.6 (c 0.13, MeOH); UV (MeOH) λ_{\max} (log ϵ) 210 (3.91) nm; ECD (MeOH, $\Delta\epsilon$) 200

(−43.442), 229 (+5.615), 294 (−5.617) nm; IR (KBr) ν_{\max} 3453, 1727, 1647, 1437, 1383, 1263 cm^{−1}; ¹H and ¹³C NMR data, see Table 1; HRESIMS m/z 621.2669 [M + Na]⁺ (calcd for C₃₃H₄₂O₁₀Na, 621.2670).

Cipadessain D (4). White powder; $[\alpha]_D^{25}$ −79.1 (c 0.13, MeOH); UV (MeOH) λ_{\max} (log ϵ) 234 (3.47) nm; ECD (MeOH, $\Delta\epsilon$) 200 (−13.199), 255 (+0.468), 294 (−3.856) nm; IR (KBr) ν_{\max} 3455, 1726, 1643, 1455 cm^{−1}; ¹H and ¹³C NMR data, see Table 1; HRESIMS m/z 591.2568 [M + Na]⁺ (calcd for C₃₂H₄₀O₉Na, 591.2565).

Cipadessain E (5). White powder; $[\alpha]_D^{25}$ −56.8 (c 0.10, MeOH); UV (MeOH) λ_{\max} (log ϵ) 208 (3.61) nm; ECD (MeOH, $\Delta\epsilon$) 200 (−22.845), 224 (+7.992), 297 (−5.732) nm; IR (KBr) ν_{\max} 3455, 1726, 1643, 1455 cm^{−1}; ¹H and ¹³C NMR data, see Table 1; HRESIMS m/z 581.2353 [M + Na]⁺ (calcd for C₃₁H₃₈O₈Na, 581.2357).

Cipadessain F (6). White powder; $[\alpha]_D^{25}$ −34.0 (c 0.09, MeOH); UV (MeOH) λ_{\max} (log ϵ) 219 (3.64) nm; ECD (MeOH, $\Delta\epsilon$) 200 (−4.342), 252 (+1.559), 296 (−3.587) nm; IR (KBr) ν_{\max} 3451, 1639, 1384, 617 cm^{−1}; ¹H and ¹³C NMR data, see Table 2; HRESIMS m/z 639.2771 [M + Na]⁺ (calcd for C₃₃H₄₄O₁₁Na, 639.2771).

Cipadessain G (7). White powder; $[\alpha]_D^{25}$ −40.1 (c 0.10, MeOH); UV (MeOH) λ_{\max} (log ϵ) 210 (3.86) nm; ECD (MeOH, $\Delta\epsilon$) 209 (−11.148), 246 (+4.267), 294 (−6.172) nm; IR (KBr) ν_{\max} 3460, 2969, 1768, 1635, 1460 cm^{−1}; ¹H and ¹³C NMR data, see Table 2; HRESIMS m/z 625.2620 [M + Na]⁺ (calcd for C₃₂H₄₂O₁₁Na, 625.2619).

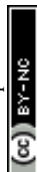
Cipadessain H (8). White, amorphous powder; $[\alpha]_D^{25}$ −54.9 (c 0.10, MeOH); UV (MeOH) λ_{\max} (log ϵ) 230 (3.35) nm; ECD (MeOH, $\Delta\epsilon$) 200 (−16.272), 224 (+7.992), 297 (−5.732); IR (KBr) ν_{\max} 3451, 2969, 1768, 1641, 1457 cm^{−1}; ¹H and ¹³C NMR data, see Table 2; HRESIMS m/z 623.2463 [M + Na]⁺ (calcd for C₃₂H₄₀O₁₁Na, 623.2464).

Cipadessain J (9). White powder; $[\alpha]_D^{25}$ −108.41 (c 0.10, MeOH); UV (MeOH) λ_{\max} (log ϵ) 213 (3.80) nm; ECD (MeOH, $\Delta\epsilon$) 200 (−20.403), 222 (+15.345) nm; IR (KBr) ν_{\max} 3400, 1725, 1645, 1460 cm^{−1}; ¹H and ¹³C NMR data, see Table 3; HRESIMS m/z 567.2597 [M − H][−] (calcd for C₃₂H₃₉O₉Na, 567.2600).

Cipadessain I (10). White powder; $[\alpha]_D^{25}$ −33.1 (c 0.10, MeOH); UV (MeOH) λ_{\max} (log ϵ) 228 (4.14) nm; ECD (MeOH, $\Delta\epsilon$) 200 (−5.196), 208 (+2.013), 225 (−5.931), 258 (+8.547), 296 (−11.285) nm; IR (KBr) ν_{\max} 3445, 1730, 1643, 1142 cm^{−1}; ¹H and ¹³C NMR data, see Table 3; HRESIMS m/z 609.2675 [M + Na]⁺ (calcd for C₃₂H₄₂O₁₀Na, 609.2670).

Cipadessain K (11). Colorless needles (MeOH–H₂O); $[\alpha]_D^{25}$ −41.5 (c 0.10, MeOH); UV (MeOH) λ_{\max} (log ϵ) 229 (3.48) nm; ECD (MeOH, $\Delta\epsilon$) 200 (+12.576), 294 (−3.937) nm; IR (KBr) ν_{\max} 3460, 2931, 1728, 1648 cm^{−1}; ¹H and ¹³C NMR, see Table 3; HRESIMS m/z 591.2565 [M + Na]⁺ (calcd for C₃₂H₄₀O₉Na, 579.2565).

X-ray crystallographic analysis of 1. Colorless crystals of **1** were recrystallized from CH₂Cl₂–MeOH (1 : 1). Crystal data were obtained on a Bruker Smart-1000 CCD with a graphite monochromator with Cu K α radiation (λ = 1.54184 Å) at 290(2) K. The structure was solved by direct methods using the SHELXS-97 (ref. 23) and expanded with difference Fourier techniques, refined with the SHELXL-97.²⁴



Crystal data of 1. $C_{32}H_{40}O_9$ ($M = 568.64$); monoclinic crystal ($0.280 \times 0.250 \times 0.200$ mm³); space group $P2_12_12_1$; unit cell dimensions $a = 1.49100$ (10) Å, $b = 13.49460$ (10) Å, $c = 18.7471$ (2) Å, $V = 2907.05$ (5) Å³, $Z = 4$, $T = 290$ (2) K, μ (Cu K α) = 0.776 mm⁻¹, $D_{\text{calc}} = 1.299$ g cm⁻³, 26 163 reflections measured ($8.072^\circ \leq 2\theta \leq 142.798^\circ$), 5564 unique ($R_{\text{int}} = 0.0242$, $R_{\text{sigma}} = 0.0160$) which were used in all calculations. The final R_1 was 0.0420 ($I > 2\sigma(I)$) and wR_2 was 0.1182 (all data). Flack parameter = -0.03 (5).

Anti-inflammatory activities

All new compounds were evaluated for their inhibitory effects on NO production in lipopolysaccharide-activated RAW 264.7 macrophages as described in the literature.²⁵ L-NMMA were used as positive control. All experiments were conducted for three independent replicates.

In vitro cytotoxicity assay

All new compounds were evaluated for their cytotoxicities against HepG₂ by MTT assay.²⁶ Cells were plated in 96-well culture plates (5×10^3 cells per well). After incubation overnight, the cells were treated with different concentrations of each compound for 48 h. DMSO (0.1%) was used as a vehicle. MTT (5 mg mL⁻¹) was dissolved in PBS and filter sterilized, then 20 µL of the prepared solution was added to each well and cells were incubated until a purple precipitate was visible. The formed formazan crystals were dissolved in DMSO (150 µL per well) by constant shaking for 10 min. The absorbance was measured on an ELISA reader (SpectraMax Plus = 384, Molecular Devices, Sunnyvale, CA) at a test wavelength of 570 nm and a reference wavelength of 630 nm. After treatment, cell viability was detected and IC₅₀ values were calculated by the Reed and Muench method.²⁶ All experiments were performed as three independent replicates.

Conflicts of interest

The authors declare no conflict of interest.

Acknowledgements

This research work was financially supported by the National Natural Science Foundation of China (31470416), the Outstanding Youth Fund of the Basic Research Program of Jiangsu Province (BK20160077), the PhD Programs Foundation of Ministry of Education of China (20120096130002), the Program for Changjiang Scholars and Innovative Research Team in University (IRT_15R63), and the Priority Academic Program Development of Jiangsu Higher Education Institutions (PAPD).

References

- S. K. Chen, B. Y. Chen and H. Li in *Zhongguo Zhiwu Zhi*, Science Press, Beijing, 1997, vol. 43, p. 58.
- S. G. Liao, H. D. Chen and J. M. Yue, *Chem. Rev.*, 2009, **109**, 1092–1140.
- Q. G. Tan and X. D. Luo, *Chem. Rev.*, 2011, **111**, 7437–7522.
- A. K. R. Bandi and D. U. Lee, *Chem. Biodiversity*, 2012, **9**, 1403–1421.
- B. Siva, B. Poominma, A. Venkanna, K. Rajendra Prasad, B. Sridhar, V. Lakshma Nayak, S. Ramakrishna and K. Suresh Babu, *Phytochemistry*, 2014, **98**, 174–182.
- X. Fang, Y. T. Di, C. S. Li, Z. L. Geng, Z. Zhang, Y. Zhang, S. Y. Yang and X. J. Hao, *J. Nat. Prod.*, 2009, **72**, 714–718.
- L. S. Gan, X. N. Wang, Y. Wu and J. M. Yue, *J. Nat. Prod.*, 2007, **70**, 1344–1347.
- Y. T. Di, P. H. He, H. Y. Liu, P. Yi, Z. Zhang, Y. L. Ren, J. S. Wang, F. W. Yang, X. Fang, S. I. Li, H. J. Zhu and X. J. Hao, *J. Nat. Prod.*, 2007, **70**, 1352–1355.
- L. G. Lin, C. P. Tang, C. Q. Ke, Y. Zhang and Y. Ye, *J. Nat. Prod.*, 2008, **71**, 628–632.
- X. Fang, Q. Zhang, C. J. Tan, S. Z. Mu, Y. Lü, Y. B. Lu, Q. T. Zheng, Y. T. Di and X. J. Hao, *Tetrahedron*, 2009, **65**, 7408–7414.
- H. J. Yu, Q. F. Liu, L. Sheng, G. C. Wang and J. M. Yue, *Org. Lett.*, 2016, **18**, 444–447.
- X. Fang, Y. T. Di, G. W. Hu, S. L. Li and X. J. Hao, *Biochem. Syst. Ecol.*, 2009, **37**, 528–530.
- J. Ning, Y. T. Di, X. Fang, H. P. He, Y. Y. Wang, Y. Li, S. L. Li and X. J. Hao, *J. Nat. Prod.*, 2010, **73**, 1327–1331.
- H. Li, Y. Li, X. B. Wang, T. Pang, L. Y. Zhang, J. Luo and L. Y. Kong, *RSC Adv.*, 2015, **5**, 40465–40474.
- X. M. Tian, H. Li, F. An, R. J. Li, M. M. Zhou, M. H. Yang, L. Y. Kong and J. Luo, *Planta Med.*, 2017, **83**, 341–350.
- Y. Li, Q. Lu, J. Luo, J. S. Wang, X. B. Wang, M. D. Zhu and L. Y. Kong, *Chem. Pharm. Bull.*, 2015, **63**, 305–310.
- T. R. Govindachari, B. Banumathy, G. Gopalakrishnan and G. Suresh, *Fitoterapia*, 1991, **70**, 106–108.
- X. Y. Wang, C. M. Yuan, G. H. Tang, T. Zou, F. Guo, J. H. Liao, H. Y. Zhang, G. Y. Zuo, G. X. Rao, Q. Zhao, X. J. Hao and H. P. He, *J. Asian Nat. Prod. Res.*, 2014, **16**, 795–799.
- M. Y. Li, X. B. Yang, J. Y. Pan, G. Feng, Q. Xiao, J. Sinkkonen, T. Satyanandamurthy and J. Wu, *J. Nat. Prod.*, 2009, **72**, 2110–2114.
- A. C. Leite, J. B. Fernandes, M. Fatima das and G. F. da Silva, *Z. Naturforsch. B*, 2005, **60**, 351–355.
- K. L. Mikolajczak, D. Weisleder, L. Parkanyi and J. Cladry, *J. Nat. Prod.*, 1988, **51**, 606–610.
- B. L. Sondengam, C. S. Kamga and J. D. Connolly, *Phytochemistry*, 1980, **19**, 2488.
- G. M. Sheldrick, SHELXS-97, *Program for Crystal Structure Resolution*, University of Göttingen, Germany, 1997.
- G. M. Sheldrick, SHELXL-97, *Program for Crystal Structure Refinement*, University of Göttingen, Germany, 1997.
- Y. S. Li, M. Ishibashi, M. Satake, X. G. Chen, Y. Oshima and Y. Ohizumi, *J. Nat. Prod.*, 2003, **66**, 696–698.
- L. J. Reed and H. A. Muench, *Am. J. Hyg.*, 1938, **27**, 493–497.

